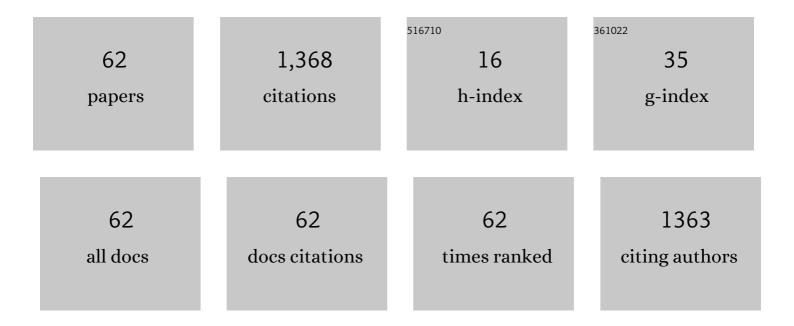
Jae-Yoon Sim

List of Publications by Year in descending order

Source: https://exaly.com/author-pdf/8049798/publications.pdf

Version: 2024-02-01



IAF-YOON SIM

#	Article	IF	CITATIONS
1	Wireless smart contact lens for diabetic diagnosis and therapy. Science Advances, 2020, 6, eaba3252.	10.3	255
2	A Fully-Integrated 71 nW CMOS Temperature Sensor for Low Power Wireless Sensor Nodes. IEEE Journal of Solid-State Circuits, 2014, 49, 1682-1693.	5.4	159
3	A 21 fJ/Conversion-Step 100 kS/s 10-bit ADC With a Low-Noise Time-Domain Comparator for Low-Power Sensor Interface. IEEE Journal of Solid-State Circuits, 2011, 46, 651-659.	5.4	139
4	A 1 GHz ADPLL With a 1.25 ps Minimum-Resolution Sub-Exponent TDC in 0.18 \$mu\$m CMOS. IEEE Journal of Solid-State Circuits, 2010, 45, 2874-2881.	5.4	118
5	A Serpentine Guard Trace to Reduce the Far-End Crosstalk Voltage and the Crosstalk Induced Timing Jitter of Parallel Microstrip Lines. IEEE Transactions on Advanced Packaging, 2008, 31, 809-817.	1.6	70
6	5.7 A 29nW bandgap reference circuit. , 2015, , .		49
7	Bimetallic Nanocatalysts Immobilized in Nanoporous Hydrogels for Longâ€Term Robust Continuous Glucose Monitoring of Smart Contact Lens. Advanced Materials, 2022, 34, e2110536.	21.0	48
8	A 192-pW Voltage Reference Generating Bandgap–\$V_{ext{th}}\$ With Process and Temperature Dependence Compensation. IEEE Journal of Solid-State Circuits, 2019, 54, 3281-3291.	5.4	46
9	A Smart Contact Lens Controller IC Supporting Dual-Mode Telemetry With Wireless-Powered Backscattering LSK and EM-Radiated RF Transmission Using a Single-Loop Antenna. IEEE Journal of Solid-State Circuits, 2020, 55, 856-867.	5.4	30
10	Inactivation of <i>S. mutans</i> Using an Atmospheric Plasma Driven by a Palm-Size-Integrated Microwave Power Module. IEEE Transactions on Plasma Science, 2010, 38, 1956-1962.	1.3	28
11	Current-Mode Transceiver for Silicon Interposer Channel. IEEE Journal of Solid-State Circuits, 2014, 49, 2044-2053.	5.4	27
12	A Single-Loop SS-LMS Algorithm With Single-Ended Integrating DFE Receiver for Multi-Drop DRAM Interface. IEEE Journal of Solid-State Circuits, 2011, 46, 2053-2063.	5.4	24
13	An 80 mV-Swing Single-Ended Duobinary Transceiver With a TIA RX Termination for the Point-to-Point DRAM Interface. IEEE Journal of Solid-State Circuits, 2014, 49, 2618-2630.	5.4	24
14	5.5 A quadrature relaxation oscillator with a process-induced frequency-error compensation loop. , 2017, , .		24
15	An 84.6-dB-SNDR and 98.2-dB-SFDR Residue-Integrated SAR ADC for Low-Power Sensor Applications. IEEE Journal of Solid-State Circuits, 2018, 53, 404-417.	5.4	24
16	A Low-Power Wide Dynamic-Range Current Readout Circuit for Ion-Sensitive FET Sensors. IEEE Transactions on Biomedical Circuits and Systems, 2017, 11, 523-533.	4.0	23
17	Smart Wireless Nearâ€Infrared Light Emitting Contact Lens for the Treatment of Diabetic Retinopathy. Advanced Science, 2022, 9, e2103254.	11.2	22
18	A 0.0043-mm ² 0.3–1.2-V Frequency-Scalable Synthesized Fractional-N Digital PLL With a Speculative Dual-Referenced Interpolating TDC. IEEE Journal of Solid-State Circuits, 2019, 54, 99-108.	5.4	16

JAE-YOON SIM

#	Article	IF	CITATIONS
19	An On-Chip Learning Neuromorphic Autoencoder With Current-Mode Transposable Memory Read and Virtual Lookup Table. IEEE Transactions on Biomedical Circuits and Systems, 2018, 12, 161-170.	4.0	15
20	A 490-pW SAR Temperature Sensor With a Leakage-Based Bandgap-Vth Reference. IEEE Transactions on Circuits and Systems II: Express Briefs, 2020, 67, 1549-1553.	3.0	14
21	36.4 A Physically Unclonable Function Combining a Process Mismatch Amplifier in an Oscillator Collapse Topology. , 2021, , .		14
22	An FFE Transmitter Which Automatically and Adaptively Relaxes Impedance Matching. IEEE Journal of Solid-State Circuits, 2018, 53, 1780-1792.	5.4	12
23	A Quadrature RC Oscillator With Noise Reduction by Voltage Swing Control. IEEE Transactions on Circuits and Systems I: Regular Papers, 2019, 66, 3077-3088.	5.4	12
24	A 2.5-nW Radio Platform With an Internal Wake-Up Receiver for Smart Contact Lens Using a Single Loop Antenna. IEEE Journal of Solid-State Circuits, 2021, 56, 2668-2679.	5.4	12
25	An Approximate Closed-Form Channel Model for Diverse Interconnect Applications. IEEE Transactions on Circuits and Systems I: Regular Papers, 2014, 61, 3034-3043.	5.4	11
26	A Study on Bandgap Reference Circuit With Leakage-Based PTAT Generation. IEEE Transactions on Very Large Scale Integration (VLSI) Systems, 2018, 26, 2310-2321.	3.1	11
27	Digitally Controlled Leakage-Based Oscillator and Fast Relocking MDLL for Ultra Low Power Sensor Platform. IEEE Journal of Solid-State Circuits, 2015, 50, 1263-1274.	5.4	10
28	A 7.8Gb/s/pin 1.96pJ/b compact single-ended TRX and CDR with phase-difference modulation for highly reflective memory interfaces. , 2018, , .		10
29	A 7.8-Gb/s 2.9-pJ/b Single-Ended Receiver With 20-Tap DFE for Highly Reflective Channels. IEEE Transactions on Very Large Scale Integration (VLSI) Systems, 2020, 28, 818-822.	3.1	8
30	A BER-Suppressed PUF With an Amplification of Process Mismatch Effect in an Oscillator Collapse Topology. IEEE Journal of Solid-State Circuits, 2022, 57, 2208-2219.	5.4	8
31	A Self-Biased Current-Mode Amplifier With an Application to 10-bit Pipeline ADC. IEEE Transactions on Circuits and Systems I: Regular Papers, 2017, 64, 1706-1717.	5.4	7
32	A 12μs-Conversion, 20mK-Resolution Temperature Sensor Based on SAR ADC. IEEE Transactions on Circuits and Systems II: Express Briefs, 2022, 69, 789-793.	3.0	7
33	An approximate condition to avoid reverse leakage current in ReRAM crossbar design. , 2015, , .		6
34	Investigation on the Worst Read Scenario of a ReRAM Crossbar Array. IEEE Transactions on Very Large Scale Integration (VLSI) Systems, 2017, 25, 2402-2410.	3.1	6
35	A Body Channel Communication Technique Utilizing Decision Feedback Equalization. IEEE Access, 2020, 8, 198468-198481.	4.2	6
36	An 18-Gb/s NRZ Transceiver With a Channel-Included 2-UI Impulse-Response Filtering FFE and 1-Tap DFE Compensating up to 32-dB Loss. IEEE Transactions on Circuits and Systems II: Express Briefs, 2020, 67, 2863-2867.	3.0	6

JAE-YOON SIM

#	Article	IF	CITATIONS
37	A PVT-Tolerant Oscillation-Collapse-Based True Random Number Generator With an Odd Number of Inverter Stages. IEEE Transactions on Circuits and Systems II: Express Briefs, 2022, 69, 4058-4062.	3.0	6
38	A Coefficient-Error-Robust Feed-Forward Equalizing Transmitter for Eye-Variation and Power Improvement. IEEE Journal of Solid-State Circuits, 2016, 51, 1902-1914.	5.4	5
39	A Low-Power Class-AB Gm-Based Amplifier With Application to an 11-bit Pipelined ADC. IEEE Transactions on Very Large Scale Integration (VLSI) Systems, 2016, 24, 2562-2569.	3.1	5
40	A 9.3 nW all-in-one bandgap voltage and current reference circuit using leakage-based PTAT generation and DIBL characteristic. , 2018, , .		5
41	A 7.8 Gb/s/pin, 1.96 pJ/b Transceiver With Phase-Difference-Modulation Signaling for Highly Reflective Interconnects. IEEE Transactions on Circuits and Systems I: Regular Papers, 2020, 67, 2114-2127.	5.4	5
42	A sample reduction technique by aliasing channel response for fast equalizing transceiver design. , 2015, , .		4
43	A Multilayer-Learning Current-Mode Neuromorphic System With Analog-Error Compensation. IEEE Transactions on Biomedical Circuits and Systems, 2019, 13, 986-998.	4.0	4
44	Increase of Power Efficiency in Coaxial Transmission Line Resonator by Using a Spacer to Compensate for Plasma Impedance. IEEE Transactions on Plasma Science, 2019, 47, 4606-4612.	1.3	4
45	Parallel Branching of Two 2-DIMM Sections With Write-Direction Impedance Matching for an 8-Drop 6.4-Gb/s SDRAM Interface. IEEE Transactions on Components, Packaging and Manufacturing Technology, 2019, 9, 336-342.	2.5	4
46	Low-Noise Distributed <i>RC</i> Oscillator. IEEE Transactions on Very Large Scale Integration (VLSI) Systems, 2022, 30, 143-152.	3.1	4
47	Analytical Formulas for Tradeoff Among Channel Loss, Length, and Frequency of <inline-formula> <tex-math notation="LaTeX">\$RC\$ </tex-math></inline-formula> - and <inline-formula> <tex-math notation="LaTeX">\$LC\$ </tex-math </inline-formula> -Dominant Single-Ended Interconnects for Fast Equalized Link Tradeoff Estimation. IEEE Transactions on Components, Packaging and Manufacturing	2.5	3
48	A Search Algorithm for the Worst Operation Scenario of a Cross-Point Phase-Change Memory Utilizing Particle Swarm Optimization. IEEE Transactions on Very Large Scale Integration (VLSI) Systems, 2018, 26, 2591-2598.	3.1	3
49	An Approximate Transfer Function Model of Two Serially Connected Heterogeneous Transmission Lines. IEEE Transactions on Circuits and Systems II: Express Briefs, 2017, 64, 1067-1071.	3.0	2
50	Microwave Plasma Generation With Resonance Frequency Tracking and Power Regulation. IEEE Transactions on Plasma Science, 2017, 45, 925-931.	1.3	2
51	A Picosecond-Resolution Digitally-Controlled Timing Generator With One-Clock-Latency at Arbitrary Instantaneous Input. IEEE Transactions on Circuits and Systems II: Express Briefs, 2020, 67, 1544-1548.	3.0	2
52	An 8.9–71.3 TOPS/W Deep Learning Accelerator for Arbitrarily Quantized Neural Networks. IEEE Transactions on Circuits and Systems II: Express Briefs, 2022, 69, 4148-4152.	3.0	2
53	Low-Power Small-Area Inverter-Based DSM for MEMS Microphone. IEEE Transactions on Circuits and Systems II: Express Briefs, 2020, 67, 2392-2396.	3.0	1
54	A DFE-Enhanced Phase-Difference Modulation Signaling for Multi-Drop Memory Interfaces. IEEE Transactions on Circuits and Systems II: Express Briefs, 2021, 68, 1862-1866.	3.0	1

JAE-YOON SIM

#	Article	IF	CITATIONS
55	A 87.5-dB-SNDR Residue-integrated SAR ADC with a Digital-domain Capacitor Mismatch Calibration. Journal of Semiconductor Technology and Science, 2021, 21, 143-151.	0.4	1
56	A 26GHz Fractional-N Digital Frequency Synthesizer Leveraging Noise Profiles of Three Functional Stages. IEEE Transactions on Circuits and Systems II: Express Briefs, 2021, 68, 3063-3067.	3.0	1
57	A 20.5-nW Resistor-Less Bandgap Voltage Reference With Self-Biased Compensation for Process Variations. IEEE Transactions on Very Large Scale Integration (VLSI) Systems, 2022, 30, 840-843.	3.1	1
58	A Time-Division Multiplexed 8-Channel Non-Contact ECG Recording IC with a Common-Mode Interference Tolerance of \$20mathrm{V}_{ext{PP}}\$. , 2022, , .		1
59	An Auto-Configurable Dual-Mode MPPT for Energy Harvesting With 12 nW–180 mW Conversion Range. IEEE Transactions on Circuits and Systems II: Express Briefs, 2022, 69, 4053-4057.	3.0	1
60	A low-power wide dynamic-range current readout circuit for biosensors. , 2018, , .		0
61	Introduction to the Special Section on the 2018 Asian Solid-State Circuits Conference (A-SSCC). IEEE Journal of Solid-State Circuits, 2019, 54, 2635-2636.	5.4	Ο
62	A 384G Output NonZeros/J Graph Convolutional Neural Network Accelerator. IEEE Transactions on Circuits and Systems II: Express Briefs, 2022, 69, 4158-4162.	3.0	0